

## Triaxial Projected Shell Model Study of $\gamma$ -deformation in atomic nuclei

G.H. Bhat<sup>1,2\*</sup>, J.A. Sheikh<sup>2</sup>, A. A. Wani<sup>1</sup> and S. Frauendorf<sup>3</sup>

<sup>1\*</sup> Department of Physics, Govt. Degree College Kulgam, 192231, India, <sup>2</sup>Cluster University Srinagar, Jammu and Kashmir, 190001, India, <sup>3</sup>Department of Physics, University of Notre Dame, Notre Dame, USA

**Abstract:** The band structures of <sup>108,112</sup>Ru isotopes are investigated using the triaxial projected shell model (TPSM) approach. It has been demonstrated that configuration mixing of various quasiparticle states can result in a dynamical change for a nucleus from being a  $\gamma$ -rigid-like to a  $\gamma$ -soft-like when interpreted in terms of the two phenomenological models of  $\gamma$ -rigid of Davydov and Filippov and  $\gamma$ -soft of Wilets and Jean. The odd-even staggering phase of the  $\gamma$  band is quite opposite in these two models and has been proposed to be an indicator of the nature of the  $\gamma$  deformation. Microscopic Triaxial Projected Shell Model has shown that the configuration mixing can lead to a transition from  $\gamma$ -rigid to  $\gamma$ -soft phases, at least, for nuclei studied in the present work.

**Key words:**  $\gamma$ -soft,  $\gamma$ -rigid, quasiparticle excitations, triaxial projected shell model.

### Introduction

Spontaneous breaking of rotational symmetry that leads to the deformation of a quantum system in the intrinsic frame, has played a pivotal role in unraveling the underlying shapes and structures of atomic nuclei [1]. The properties of deformed nuclei are elucidated by considering the ellipsoidal shape, which is conveniently parameterized in terms of axial and non-axial deformation parameters of  $\beta$  and  $\gamma$ . The majority of the deformed nuclei are axially-symmetric ( $\gamma = 0$ ) with angular-momentum projection along the symmetry axis,  $K$ , a conserved quantum number and the electromagnetic transition probabilities obeying the selection rules based on this quantum number [2,3]. There are also regions in the nuclear periodic table, referred to as transitional, where the axial symmetry is broken and the non-axial degree of freedom plays an essential role in determining the properties of these nuclei. Atomic nuclei may have either a localized minimum or a flat

potential energy surface along the  $\gamma$  degree of freedom and correspond to  $\gamma$ -rigid and  $\gamma$ -soft nuclei, respectively [4,5,6,7]. How to distinguish between the two shapes from the observable properties has been an outstanding issue in nuclear physics for more than sixty years. It is known that Davydov-Filippov and Wilets-Jean potentials belonging to  $\gamma$ -rigid and  $\gamma$ -soft limits, respectively, give rise to similar excitation spectra for the ground-state band [8,9]. It is, therefore, impossible to delineate the two shapes from the ground-state properties for which rich data is available for most of the nuclei. Nevertheless, it has been demonstrated that energy staggering in the  $\gamma$ -band may shed light on the nature of the  $\gamma$ -motion. For  $\gamma$ -soft nuclei described by Wilets-Jean potential, the energies of the  $\gamma$ -band are bunched as  $(2^+)$ ,  $(3^+, 4^+)$ ,  $(5^+, 6^+)$ ..... and in the Davydov-Filippov model corresponding to the  $\gamma$ -rigid limit, the energy levels of the  $\gamma$ -band are arranged as  $(2^+, 3^+)$ ,  $(4^+, 5^+)$ ,  $(6^+, 7^+)$ ..... The sequence of the energy levels of the  $\gamma$ -band leads to opposite phase of the staggering parameter in the two cases.

\*Corresponding author(s):  
gwhr.bhat@gmail.com (G. H. Bhat)

The purpose of the present work is to investigate the  $\gamma$ -band staggering in even-even nuclei using the microscopic triaxial projected shell model (TPSM) approach [10]. The study is performed for  $^{108, 112}\text{Ru}$  nuclei for which  $\gamma$ -bands are observed up to high angular momentum for both even- and odd-spin members. It is demonstrated that angular-momentum projection from the intrinsic triaxial vacuum or 0-quasiparticle state in the TPSM approach gives rise to  $\gamma$ -band staggering corresponding to Davydov-Filippov model or rigid- $\gamma$  motion. However, it is demonstrated that inclusion of quasiparticle excitations transforms the  $\gamma$ -band staggering from Davydov-Filippov kind to what is expected from Wilets-Jean or  $\gamma$ -soft motion for  $^{108}\text{Ru}$  nucleus while for  $^{112}\text{Ru}$  the situation is reversed. In the following, we shall first briefly describe the TPSM approach before discussing the results.

### Outline of Triaxial Projected Shell Model

The basic theory of the applied framework, Triaxial Projected Shell Model (TPSM), is presented briefly in the current section. A detailed systematics of TPSM or PSM and its computational coding has been provided by JAS, G. H. Bhat, Hara and Sun [15,20,21]. The central achievement of TPSM is to provide interpretation of results in the simple physical terms. The TPSM uses a novel and efficient way to bridge the two conventional methods: the deformed mean-field approximations, which are widely applied to heavy nuclei, but able to describe the physics only in the intrinsic frame, and the spherical shell model diagonalization method, which is most fundamental but feasible only for small systems. Furthermore, it is possible to detect extremely delicate and fine structural features

of the nuclei present in the Segre chart with PSM.

The many-body valence space in the TPSM begins with the deformed (Nilsson-type) single particle basis as the use of spherical shell model basis makes no sense for the deformed nuclei. Pairing correlation is incorporated by successive BCS calculations for the Nilsson single particle basis. The size of the basis, so obtained, is determined by quasi-particle ( $qp$ ) energy truncation, typically 2 MeV above and below the Fermi energy. While constructing single particle intrinsic states, rotational symmetry is broken which is restored by the projection technique [30]. The single particle configuration contains three major shells (N) for both protons as well as neutrons. In the TPSM, the states of eve-even nuclei constructed by 0-qp state (or qp-vacuum  $|\Phi\rangle$ ), 2-neutron, 2-proton and 4-qp configurations. The multi-quasi-particle states ( $|\phi_k\rangle$ ) are spanned by the set,

$$|\phi_k\rangle = \{|0\rangle, a_{\pi 1}^\dagger a_{\pi 2}^\dagger |0\rangle, a_{\nu 1}^\dagger a_{\nu 2}^\dagger |0\rangle, a_{\pi 1}^\dagger a_{\pi 2}^\dagger a_{\nu 1}^\dagger a_{\nu 2}^\dagger |0\rangle\} \quad (1)$$

For even-even nuclei, where  $|0\rangle$  is the Nilsson + BCS quasi-particle vacuum.  $a^\dagger$ 's are the quasi-particle creation operators for this vacuum and  $\nu$ 's ( $\pi$ 's) denote the neutron (proton) Nilsson quantum numbers which run over the quasi-particle vacuum or zero quasi-particle state.

In the TPSM, the many-body wave function is a superposition of (angular momentum) projected multi-quasi-particle states. Angular momentum projection transforms the wave function from the intrinsic frame to the laboratory frame. The total wave function is expressed as

$$|\Psi_{IM}^\sigma\rangle = \sum_{K\kappa} f_K^\sigma \hat{P}_{MK}^I |\phi_\kappa\rangle, \quad (2)$$

with  $\hat{P}_{MK}^I = \frac{2I+1}{8\pi^2} \int d\Omega D_{MK}^I(\Omega) \hat{R}(\Omega)$

where, the index  $\sigma$  labels the states with same angular momentum and  $\kappa$  labels the basis states.

$\hat{P}_{MK}^I$  is the angular momentum projection operator [19] and  $f_K^\sigma$  are the weights of the basis state  $\kappa$ . Further,  $\hat{R}(\Omega)$  being the rotation operator and  $D_{MK}^I(\Omega)$  the corresponding matrix. It is worth to mention here that the triaxial vacuum configuration is a superposition of K-configurations and it can be easily shown that only even-K values are permitted due to symmetry requirement. The projected bands from the vacuum state with  $K=0, 2$  and  $4$  in the D-matrix result into ground-,  $\gamma$ - and  $\gamma\gamma$ -bands, respectively. For two-quasiparticle states, both even- and odd-K values are permitted depending on the nature of the quasiparticles. For a two quasiparticle configuration formed from normal and time-reversed states, only even-K are permitted. However, with both the states either normal or time-reversed, odd-K values are allowed from symmetry considerations.

The energies and wave functions (given in terms of the coefficients  $f_K^\sigma$  in Eq. (2)) are obtained by solving the following eigen-value equation

$$\sum_{K'} \{H_{K\kappa K'}^I - E_I^\sigma N_{K\kappa K'}^I\} f_{K'}^\sigma = 0 \quad (3)$$

where,  $H_{K\kappa K'}^I$  and  $N_{K\kappa K'}^I$  are respectively the matrix elements of the Hamiltonian and the norm and are given as

$$H_{K\kappa K'}^I = \langle \phi_\kappa | \hat{H} \hat{P}_{K\kappa K'}^I | \phi_{\kappa'} \rangle \text{ and} \\ N_{K\kappa K'}^I = \langle \phi_\kappa | \hat{P}_{K\kappa K'}^I | \phi_{\kappa'} \rangle \quad (4)$$

The projection of an intrinsic state  $|\phi_k\rangle$  on a good angular momentum generates a rotational energy of a band (or the band energy)

$$E_K(I) = \frac{\langle \phi_\kappa | \hat{H} \hat{P}_{K\kappa K}^I | \phi_\kappa \rangle}{\langle \phi_\kappa | \hat{P}_{K\kappa K}^I | \phi_\kappa \rangle} = \frac{H_{K\kappa K}^I}{N_{K\kappa K}^I} \quad (5)$$

which can be plotted as a function of spin for various bands and important physics can be drawn from these plots.

The rotationally invariant Hamiltonian used in the present TPSM calculations is taken as

$$\hat{H} = \hat{H}_0 - \frac{1}{2} \chi \sum_\mu \hat{Q}_\mu^\dagger \hat{Q}_\mu - G_M \hat{P}^\dagger \hat{P} - G_Q \sum_\mu \hat{P}_\mu^\dagger \hat{P}_\mu \quad (6)$$

In the above equation,  $H_0$  represents the spherical single particle shell model Hamiltonian, involving spin-orbit interactions whose strengths are the Nilsson parameters denoted by  $\kappa$  and  $\mu$ . The second term in the Hamiltonian is the quadrupole-quadrupole (Q-Q) interaction and the last two terms denote the monopole and quadrupole pairing interactions, respectively. The strength of these two-body quadrupole interactions is described by the parameter  $\chi$  which is adjusted so that quadrupole deformation  $\varepsilon_2$  is obtained. However, the monopole pairing strength, which was first introduced by Dieterich et al., [31] takes the form

$$G_M = \left( G_1 \mu G_2 \frac{N-Z}{A} \right) \frac{1}{A} \quad (\text{MeV})$$



where the - (+) sign is for neutrons (protons), The choice of the strengths  $G_1$  and  $G_2$  depends on the size of the single particles gaps in the calculations. The quadrupole pairing strength,  $G_Q$ , is supposed to be proportional to  $G_M$ . Finally, a two-body shell model Hamiltonian is diagonalized in the projected basis. By the diagonalization of the Hamiltonian, given by Eq. (6), in the projected

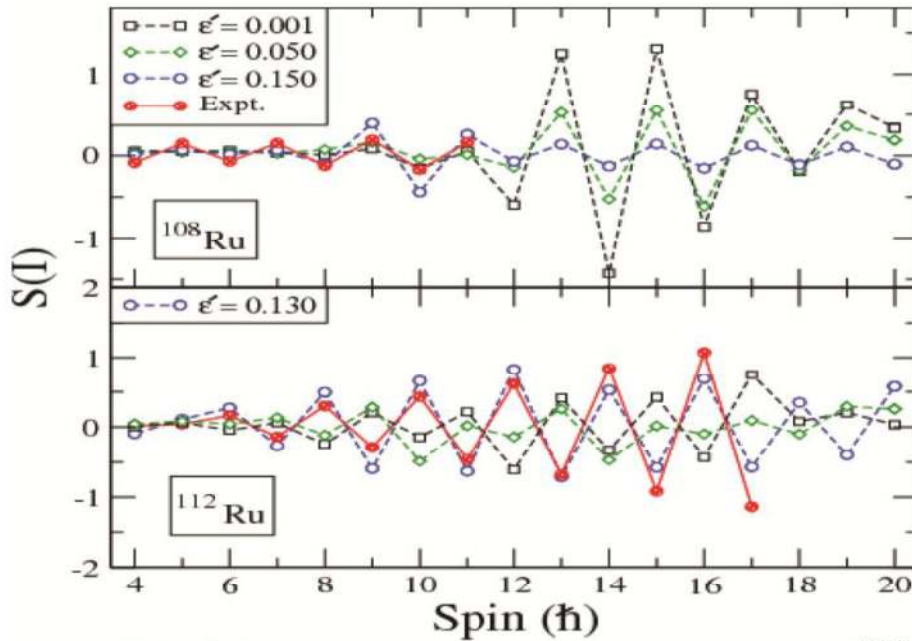


Fig. 1. (Coloronline) Comparison of experimental and the calculated band energies for  $^{108,112}\text{Ru}$ .

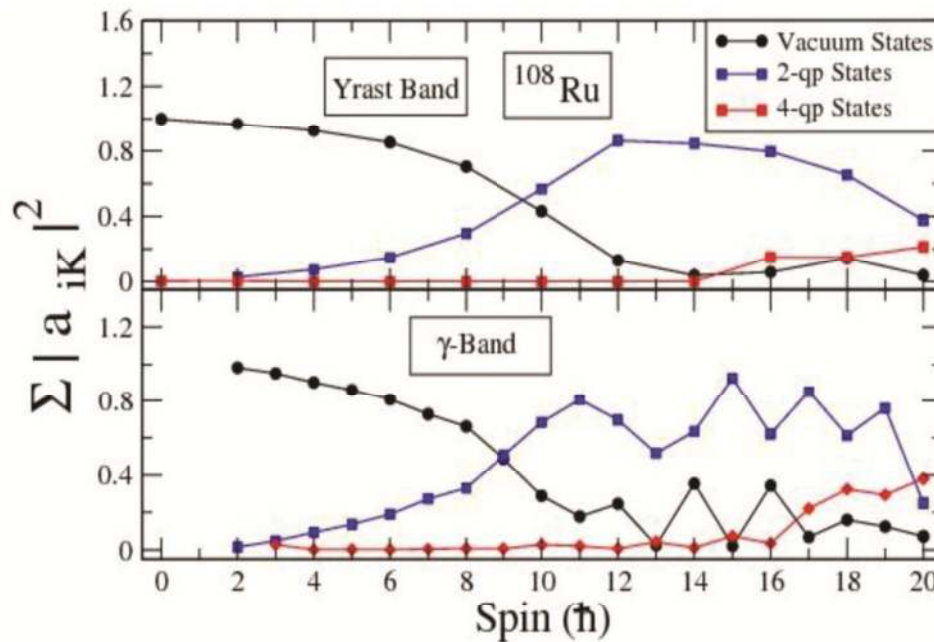


Fig. 2. (Color online) Probability of various projected K-configurations in the wave-functions of the excited bands in  $^{108}\text{Ru}$ . For clarity, only the lowest projected K-configurations in the wavefunctions of bands are shown and in the numerical calculations, projection has been performed from more than forty intrinsic states. In the Fig. the average amplitudes are plotted for each configuration.

$G_2$  depends on the size of the single particles gaps in the calculations. The quadrupole pairing strength,  $G_Q$ , is supposed to be proportional to  $G_M$ . Finally, a two-body shell model Hamiltonian is diagonalized in the

bases, given by Eq. (1), one thus obtains energy levels for a given spin. The final results come from diagonalizing a two-body Hamiltonian in the projected basis, and consequently involve fluctuations between the deformed and pairing

fields. The interaction strengths used are consistent with those used in our earlier studies [13,14,15,16,17,18,19].

## Results and Discussion

TPSM study has been performed for Ru isotopes. Deformation parameters of  $\epsilon$  ( $\epsilon'$ ) employed in the TPSM calculations are 0.294(0.140) and 0.290(0.150) for  $^{108}\text{Ru}$  and  $^{112}\text{Ru}$  respectively. The axial deformation parameter is either fixed such the observed quadrupole moment of the first excited state is reproduced or from other theoretical studies. On the other hand, the non-axial parameter,  $\epsilon'$ , is determined such that the band-head of the  $\gamma$ -band is reproduced. There are other ways of choosing this parameter, for instance, from the minimum of the potential energy surface with  $\epsilon'$  as a generator coordinate. However, it has been shown in our earlier work that this leads to similar non-axial deformation value as that deduced through fixing the band-head of the  $\gamma$ -band.

Analyzing the collective Bohr-Hamiltonian results, it has been suggested that signature splitting of the  $\gamma$ -band is sensitive to the nature of  $\gamma$ -deformation. The observed pattern is as follows: for harmonic  $\gamma$ -vibration about an axial shape, both signatures are degenerate; for a  $\gamma$ -independent potential, even spin is below odd spin; for a rigid triaxial potential, odd spin is below even spin. To quantify the tendency, the following staggering parameter has been introduced:

$$S(I) = \frac{E(I) - [E(I-1) + E(I+1)]}{E(2_1^+)}$$

which measures the energy of state  $I$  relative to the average energy of the two neighbours. The staggering  $S(I)$  is quite small at low-spin, which is expected for a well established axial shape.

Above  $I = 10$  the staggering increases, with the even-spin states below the odd ones. Further, to probe the dependence of the  $\gamma$ -band staggering on the triaxial deformation parameter, in Fig. 1  $S(I)$  is displayed for  $^{108}\text{Ru}$  and  $^{112}\text{Ru}$  with different values of  $\epsilon'$ . It is noted from Fig. 1 that the phase of  $S(I)$  remains unchanged for  $^{108}\text{Ru}$  as the motion is  $\gamma$ -soft and any value of  $\epsilon'$  can be chosen to reproduce the phase of the staggering. On the other hand, it is observed that in order to reproduce the observed phase for the  $\gamma$ -band in  $^{112}\text{Ru}$ , the triaxial deformation value of  $\epsilon' = 0.13$  ( $\gamma = 24^\circ$ ) is needed. What emerges from the above discussion is that  $^{112}\text{Ru}$  is a unique nucleus for which phase of the staggering for all spin states remains that of Davydov-Filipov kind even after considering quasiparticle excitations. For other  $^{108}\text{Ru}$  nucleus, the phase of the staggering changes, atleast, for some spin states with the inclusion of the quasiparticle states. Thus, from the present analysis,  $^{112}\text{Ru}$  can be considered as a truly  $\gamma$ -rigid nucleus. The question that naturally arises is what is the magnitude of the quasiparticle configurations in  $^{112}\text{Ru}$  as compared to a  $\gamma$ -soft nucleus. In order to address this question, the wavefunction amplitudes are plotted for  $^{108,112}\text{Ru}$  isotopes in Fig. 2 and 3. These wavefunction amplitudes indicate that in  $^{108}\text{Ru}$ , both yrast and  $\gamma$  bands are dominated by the vacuum configuration up to  $I=8$  and above this spin value the two-quasiparticle configurations dominate. This is due to the well established crossing of the two-quasiparticle aligned band with the ground-state band.

For  $^{112}\text{Ru}$ , the only difference as compared to  $^{108}\text{Ru}$  is that crossover occurs at  $I=10$  rather than at  $I=8$ . In particular, the magnitude of the two-quasiparticle amplitude is very similar in two nuclei.

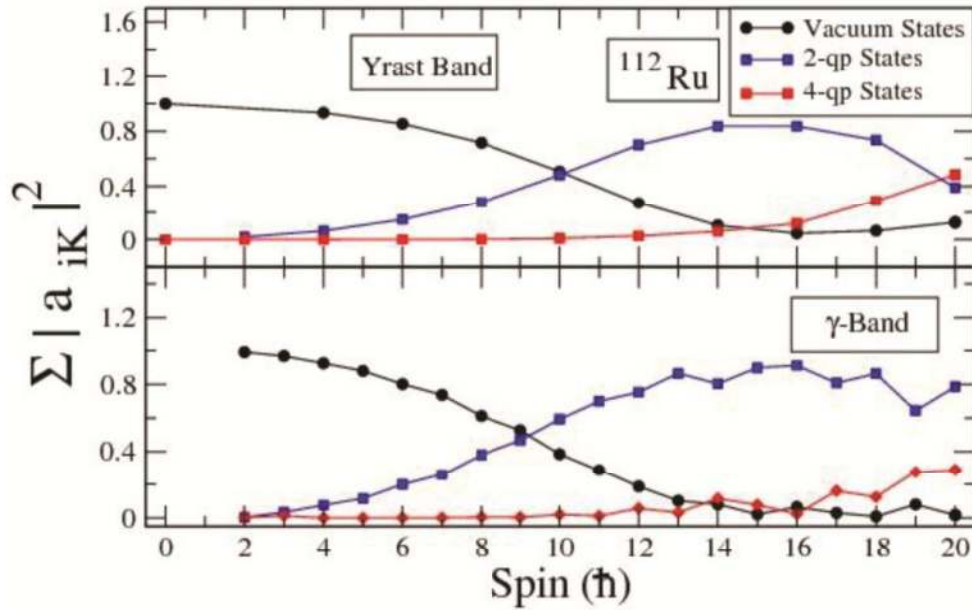


**Fig. 3.** (Color online) Probability of various projected K-configurations in the wave-functions of the excited bands in  $^{112}\text{Ru}$ . For clarity, only the lowest projected K-configurations in the wavefunctions of bands are shown and in the numerical calculations, projection has been performed from more than forty intrinsic states. In the Fig. the average amplitudes are plotted for each configuration.

## Conclusion

In conclusion, It would have been normally expected that due to smaller contribution from quasiparticle excitations,  $^{112}\text{Ru}$  maintains the  $\gamma$ -rigid motion of the vacuum state. Therefore, the reason for the  $\gamma$ -rigid motion in  $^{112}\text{Ru}$  appears to be more deeper and is rooted in the basic shell structure of nucleus.

## Acknowledgements

We would like to express our deep gratitude to Prof. R. Palit (Tata Institute of Fundamental Research, Colaba, Mumbai, 400 005, India), Prof. Yang Sun (Department of Physics, University of Notre Dame, Notre Dame, IN 46556, USA) and S. Jehangir (National Institute of Technology, Srinagar, 190 006, India) for their contributions at various stages in the development of the triaxial projected shell model approach.

## References

- [1] S. Frauendorf, *Rev. Mod. Phys.* **73**, 463 (2001).
- [2] S. G. Nilsson, *Dan. Mat. Fys. Medd.* **29**, 16 (1955).
- [3] A. Bohr and B. R. Mottelson, *Nuclear Structure, Vol. II* (Benjamin Inc., New York, 1975).
- [4] N. V. Zamfir and R. F. Casten, *Phys. Lett.* **B 3**, 260 (1991).
- [5] A. S. Davydov, in: *Proc. Intern. Conf. on Nuclear structure* (Kingston, Canada), eds. D.A. Bromley and E.W. Vogt (University of Toronto Press, Toronto, 1960) p. 801
- [6] K. Kumar, *Phys. Rev. C* **1**, 369 (1970).
- [7] C. Baktash et al., *Phys. Rev. C* **18**, 131 (1978); **C 22**, 2383 (1980).



- [8] A.S. Davydov and G. P. Filippov, Nucl. Phys. **8**, 237 (1958).
- [9] L. Wilets and M. Jean, Phys. Rev. **102**, 788 (1956).
- [10] J. A. Sheikh and K. Hara, Phys. Rev. Lett. **82**, 3968 (1999).
- [11] P. Ring and P. Schuck, The Nuclear Many Body Problem (Springer-Verlag, New York), (1980).
- [12] S. G. Nilsson, C. F. Tsang, A. Sobiczewski, Z. Szymanski, S. Wycech, C. Gustafson, I. Lamm, P. Moller, and B. Nilsson, Nucl. Phys. **A 131**, 1 (1969).
- [13] G. H. Bhat, W. A. Dar, J. A. Sheikh, and Y. Sun, Phys. Rev. **C 89**, 014328 (2014).
- [14] C. L. Zhang, G. H. Bhat, W. Nazarewicz, J. A. Sheikh, and Yue Shi, Phys. Rev. **C 92**, 034307 (2015).
- [15] J. A. Sheikh, G. H. Bhat, Y. Sun, G. B. Vakil, and R. Palit, Phys. Rev. **C 77**, 034313 (2008).
- [16] J. A. Sheikh, G. H. Bhat, R. Palit, Z. Naik, and Y. Sun, Nucl. Phys. **A 824**, 58 (2009).
- [17] S. Jehangir, G. H. Bhat, J. A. Sheikh, S. Frauendorf, S. N. T. Majola, P. A. Ganai, and J. F. Sharpey-Schafer, Phys. Rev. **C 97**, 014310 (2018).
- [18] J. A. Sheikh, G. H. Bhat, Y.-X. Liu, F.-Q. Chen, and Y. Sun, Phys. Rev. **C 84**, 054314 (2011).
- [19] G. H. Bhat, J. A. Sheikh, Y. Sun, and U. Garg, Phys. Rev. **C 86**, 047307 (2012).
- [20] K. Hara, Y. Sun, Int. J. Mod. Phys. **E 4** (1995) 637.
- [21] Y. Sun, K. Hara, Comput. Phys. Commun. **104** (1997) 245.